

# Capacitive detection of the topological magnetoelectric effect

Chao Lei<sup>1,\*</sup>, Perry T. Mahon<sup>1</sup>, C. M. Canali<sup>2</sup>, and A. H. MacDonald<sup>1</sup>

<sup>1</sup>Department of Physics, University of Texas at Austin, Austin, Texas 78712, USA and

<sup>2</sup> Department of Physics and Electric Engineering, Linnaeus University, 392 31 Kalmar, Sweden

(Dated: June 18, 2024)

The topological magnetoelectric effect (TME) is a defining property of 3-dimensional  $\mathbb{Z}_2$  topological insulators that was predicted on theoretical grounds more than a decade ago, but has still not been directly measured. In this Letter we propose a strategy for direct measurement of the TME, and discuss the precision of the effect in real devices with charge and spin disorder.

*Introduction*— The (electronic) ground state of 3-dimensional (3D) time-reversal invariant band insulators can be classified by a  $\mathbb{Z}_2$  index [1–5]. In thin films of  $\mathbb{Z}_2$ -odd materials, the nontrivial bulk topology implies the existence of an odd number of surface state Dirac cones that are commonly revealed by angle-resolved photoemission spectroscopy [6–8]. One key property [1, 9] of bulk  $\mathbb{Z}_2$  topological insulators (TIs) is the quantization of their magnetoelectric response. The formal bulk response manifests as an observable topological magnetoelectric effect (TME) only when the surface states are gapped by locally breaking time-reversal so that they support a surface Hall conductivity [1, 9–20]. Although first proposed more than 15 years ago, the TME has not been yet directly measured. In this Letter we discuss why the observation of the TME has been difficult, propose a strategy for its measurement, and speculate on the precision of the effect’s quantization in real samples with disorder.

Magnetoelectric response refers to the linear response of (electronic) polarization  $\mathbf{P}$  in a dielectric to a uniform dc magnetic field  $\mathbf{B}$  or equivalently to the linear response of orbital magnetization  $\mathbf{M}$  to a uniform dc electric field  $\mathbf{E}$  and is described by the susceptibility tensor

$$\alpha^{il} = \left. \frac{\partial P^i}{\partial B^l} \right|_{\mathbf{E}=\mathbf{0}} = \left. \frac{\partial M^l}{\partial E^i} \right|_{\mathbf{B}=\mathbf{0}}. \quad (1)$$

The TME of a  $\mathbb{Z}_2$ -odd TI refers to a response tensor that is diagonal and quantized:  $\alpha^{il} = \delta_{i,l}(2n+1)e^2/2hc$  for some  $n \in \mathbb{Z}$ , where  $2n+1$  is the number of Dirac cones. For concreteness, we focus below on  $\mathbb{Z}_2$ -odd thin film with one Dirac cone at each surface for which  $n=0$  (realized *e.g.* in  $\text{Bi}_2\text{Te}_3$ ), but our conclusions are valid more generally. In realistic samples, the TME is accurately quantized only when the sample is large [18, 20, 21]. Because the TME has never been measured directly, little is known with confidence about how it is changed by the inevitable disorder present in realistic devices.

In this Letter we propose a simple strategy for measuring the TME of non-magnetic TI thin films with magnetic dopants at top and bottom surfaces. In the thin film geometry, the TME occurs only when the two film surfaces have opposite magnetization orientations. This enabling configuration of the TI thin film magnetization is referred to as the axion configuration [1, 16, 22] because of an analogy between the electrodynamics implied by the TME and axion field theories [23]. When the two surface magnetizations are parallel, the system

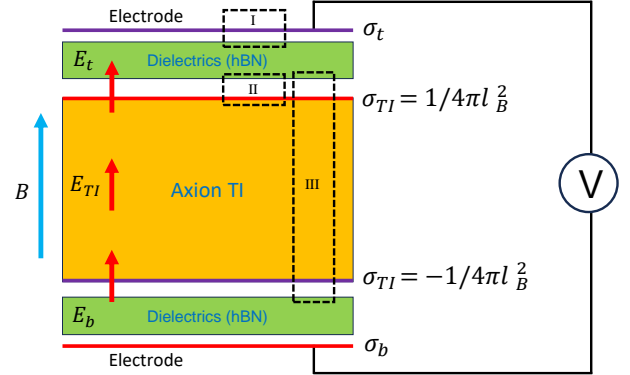


FIG. 1. Measurement scheme for the magnetoelectric coefficient  $\alpha$  of  $\mathbb{Z}_2$  TI thin films. A floating  $\mathbb{Z}_2$  TI film with surface magnetizations in an axion configuration (see main text) is encapsulated by hexagonal boron nitride (hBN) and placed between two parallel electrodes. The van der Waals stack therefore acts as a compound dielectric in a planar capacitor. When a magnetic field is applied, the topological magnetoelectric effect is manifested by the accumulation of charges on the two TI surfaces with areal densities  $\pm 1/4\pi l_B^2$  (assuming there is a single Dirac cone at each surface), where  $l_B$  is the magnetic length. The TI surface densities add an offset of  $\pm C_{TI}^{-1} A \alpha_{me} B$  to the capacitance voltage at fixed electrode charge. The sign of the surface densities is related to the magnetic configuration at each surface, and for concreteness in this figure we have assumed magnetic surface dopants aligned parallel to the surface normal.

has a quantum Hall effect (QHE) [24] that induces chiral edge states which cross the Fermi level and violate the fixed charge condition needed to define polarization in a dielectric. The TME measurement scheme we propose employs a floating sandwich structure, with two non-magnetic  $\mathbb{Z}_2$ -even dielectric layers (*e.g.*, hexagonal boron nitride (hBN)) separating the TI sample from gates as shown in Fig. 1. The polarization induced by an external uniform dc magnetic field that is parallel to the surface normal of the thin film leads to an accumulated charge density  $\pm 1/4\pi l_B^2$  at the top and bottom surfaces of an axion configured TI, which can be detected by measuring the magnetic field dependence of the capacitor voltage at fixed charge as explained below.

*Capacitive TME Measurement Scheme*— As illustrated in Fig. 1, when a uniform dc magnetic field  $\mathbf{B}$  is applied to a non-magnetic TI thin film with an axion magnetic dopant configuration, electric polarization is induced and manifested

by surface charge densities of opposite sign on top and bottom surfaces. Electrical measurement of these surface charge densities is subtle because the currents that cause the surface charge densities to accumulate cannot be measured externally [18]. Instead, the surface charges result from internal currents that flow as the parameters of an isolated equilibrium system are varied [10]. Our goal in the following is to explain an electrical measurement scheme that can verify quantization if it is realized. The basic idea is to avoid direct electrical contact to the TI, which sits in the interior of the capacitor's dielectric stack, in order to ensure its total charge neutrality (see Fig. 1). We apply Gauss's law

$$\oint_S \epsilon \mathbf{E} \cdot d\mathbf{A} = 4\pi Q, \quad (2)$$

where  $Q = eA\sigma$  is the total *free* charge [25] enclosed by a general surface  $S$ ,  $e$  is the elementary charge, and  $A$  is the cross-sectional area of the device, to the Gaussian surfaces in Fig. 1. For example, by usual electrostatics arguments, application to box *I* yields

$$E_t = 4\pi e\sigma_t/\epsilon_t \quad (3)$$

for the electric field in the top dielectric layer due to  $\sigma_t$ , where  $\sigma_t$  is the charge density on the top electrode and  $\epsilon_t$  is the dielectric constant of the top dielectric material (e.g., hBN). When we apply Gauss's law to box *II*, which includes the top surface of the axion configured TI, we obtain

$$\epsilon_t E_t - \epsilon_{TI} E_{TI} = 2\pi e(1 + \delta)B/\Phi_0. \quad (4)$$

Here  $\Phi_0 = hc/e$  is the Dirac magnetic flux quantum and  $\delta$  is included to account for any deviations of the magnetoelectric response from the expected quantized value, which could be produced by disorder as we discuss below. Finally, applying Gauss's law to box *III* implies that the electric fields in the top and bottom dielectrics are identical, as required by the charge neutrality of the floating TI film. The total voltage drop across the dielectric stack is therefore  $V = E_t d_t + E_b d_b + E_{TI} d_{TI}$ , which we write as

$$V = s C_{TI}^{-1} A \alpha_{me} B + C_g^{-1} Q. \quad (5)$$

Here  $\alpha_{me} = (e/2)(1 + \delta)/\Phi_0$ ,  $|s| = 1$  in axion insulator magnetic configurations and changes sign between upsweep and downsweep (see below), whereas  $s = 0$  in the quantum anomalous Hall magnetic configurations. In Eq. 5  $C_g^{-1} \equiv 4\pi \sum_j d_j/(\epsilon_j A)$  is the total geometric capacitance,  $d_j$  is the thin film thickness for  $j = t, b, TI$ , and  $C_{TI}^{-1} \equiv 4\pi d_{TI}/(\epsilon_{TI} A)$  is the geometric capacitance of the TI. The topological magnetoelectric coefficient can therefore be extracted by measuring the voltage across the device as an external magnetic field that is parallel to the surface normal is varied.

*Capacitive Hysteresis Loop*— In Fig. 2 we illustrate how the capacitor's voltage varies at fixed charge across a perpendicular field magnetic hysteresis loop. The geometric capacitance and electrode area are device-dependent quantities.

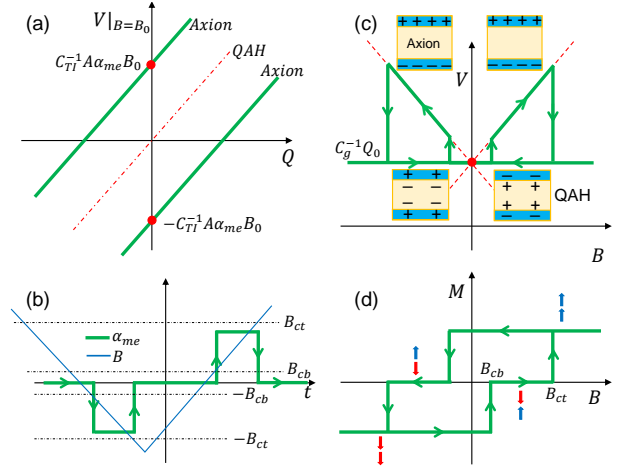


FIG. 2. (a) Dependence of  $V|_{B=B_0}$  on capacitance charge  $Q$  in QAH and axion insulator magnetic surface dopant configurations. The top (bottom) curve applies to axion configurations with surface magnetic moments parallel (anti-parallel) to the surface normal. The middle (bottom) curve applies to QAH configurations. (b) Time  $t$  variation of magnetic field (blue curve) in the proposed hysteresis loop and the magnetoelectric coefficient (green curve) of the electronic state (QAH or axion) expected at time  $t$  when the two surface magnets switch at different coercive fields  $B_{ct} < B_{cb}$  and the field is swept slowly. (c) Voltage drop across the dielectric stack during the proposed hysteresis loop at a fixed electrode charge  $Q_0$  (described in main text). (d) Surface magnetic configuration during the proposed hysteresis loop. Because the top surface coercive field is assumed to be smaller, the parallel axion configuration appears in the upsweep branch of the hysteresis loop and the anti-parallel configuration on the downsweep branch.

The dependencies of capacitance voltage on electrode charge when the external magnetic field is fixed at  $B_0$  in axion insulator and quantum anomalous Hall (QAH) states are illustrated in Fig. 2(a). Here all curves have slope  $C_g^{-1}$  and the TME is manifested by offset voltages  $\pm C_{TI}^{-1} A B_0 \alpha_{me}$  in the two axion magnetic configurations. The TME is reflected most directly when  $B$  is varied across a hysteresis loop. We assume that the magnets formed by the two surface dopant systems are weakly exchange coupled and that they have different coercive fields. We start the hysteresis loop from positive fields  $B$  that exceed both coercive fields  $B_{c,t/b}$  such that the magnetizations on top and bottom surfaces are aligned. Thus, the system begins in a QAH state. We then follow the field loop summarized in Fig. 2(b). According to the Streda formula [26–29], the charge density at which the gap appears is non-zero at finite magnetic field in a quantum anomalous Hall state. The thin film, which is neutral, must therefore have a Fermi level outside the gap and behave as a metal in the sense of fully screening the external field deep in its bulk, reducing its contribution to the voltage compared to the dielectric contribution contained in  $C_g^{-1}$ . This reduction, which we do not expect to be a large contribution to the total voltage, will decrease in magnitude as the magnetic field strength is reduced toward zero. For a sufficiently negative  $B$  one of the two surface magnetizations

( $t$  for instance) will flip, converting the magnetic configuration from QAH to axion. It is at this point that the topological insulator surfaces first develop the opposite charge densities related to the TME, and these make the contribution to the voltage proportional to  $\alpha_{me}B$  (see Fig. 2(c)). At stronger negative values of  $B$ , both coercive fields are exceeded the magnetic configuration is converted back to QAH. This QAH state will have the opposite sign of surface magnetization and Hall conductivity compared to the starting state (see Fig. 2(d)). The axion state induced on the upsweep part of the hysteresis loop has the same sign of incremental voltage as on the downsweep because both the magnetoelectric coefficient and the magnetic field have changed sign.

The absolute value of the TME effect is likely most reliably extracted from the size of the voltage jumps that occur near the reversal points in the magnetic hysteresis loop, or equivalently from the currents that would flow through the external circuit to change the capacitor charge if the voltage was held fixed. The relative correction to quantization  $\delta$  is related to the measured voltage jump  $\Delta V$

$$1 + \delta = \frac{2C_{TI}\Phi_0}{eAB^*} |\Delta V|, \quad (6)$$

where  $B^*$  is the magnitude of the field (equal to the top or bottom layer coercive field) at which the jump occurs. Expressed in natural units, the voltage jump  $|\Delta V| \approx 2.18(1 + \delta)d_{TI}B^*/\epsilon_{TI}$  in units of mV when  $d_{TI}$  is expressed in units of nm and  $B^*$  in units of T. For  $\epsilon_{TI} = 10$ ,  $B^* = 1T$ ,  $d_{TI} = 10nm$ ,  $|\Delta V|$  is therefore around 2.18(1 +  $\delta$ ) mV. Extracting  $\delta$  requires knowledge of the capacitance of the TI, But this quantity can be measured for the same sample under the same experimental conditions by using the total capacitance at  $B = 0$  in the hysteresis loop and accounting for the inverse capacitance contributions from the hBN dielectric layers. It is desirable to keep the dielectric layers thin in order that this correction, which needs to be estimated from known dielectric constants and sample thicknesses, is relatively small. Due to this correction, the parts per millions accuracy routinely achieved in quantum Hall effect measurements seems out of reach. However this measurement accuracy may be irrelevant since we do not expect that the effect will be realized accurately in realistic devices with disorder, as we now explain.

*Effect of Disorder on the Precision of TME Quantization—* In order to begin a discussion of the influence of disorder on TME quantization accuracy, we comment on the physical processes taking place when the hysteresis loop is transited. The voltage jumps that take place at negative  $B$  on the downsweeps and at positive  $B$  on the upsweeps occur as the local magnetization direction on either the top or bottom surface is in the process of reversing. These changes in surface magnetization drive anomalous currents that flow through the bulk of the film [20, 30]. On the other hand, the steady rate of voltage change that occurs after the magnetization has completely reversed is due [21] to charges that flow between surfaces on the side-walls. In both cases, the change in charge distribution across the film is a purely equilibrium phenomena.

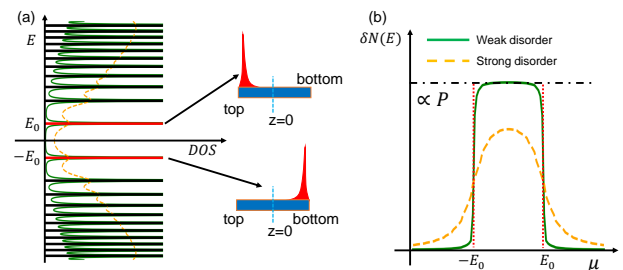


FIG. 3. Anomalous Landau levels and the effect of disorder. (a) Effect of disorder on the density of states (DOS): the left panel plots the DOS vs. band energy with and without disorder, with the green (orange dashed) curves for weak (strong) disorder. (b) Difference between the electronic densities in the top and bottom ( $\delta N(E)$ ) halves of a finite thickness  $\text{Bi}_2\text{Te}_3$  film for weak and strong disorder vs. chemical potential. When there is weak disorder there is a charge gap at neutrality and  $\delta N(E)$  is maximized for chemical potentials in this gap. The size of the energy gap is bounded by that of the  $N = 0$  LL in the system with no disorder (denoted  $2E_0$ ). When there is strong disorder there is no charge gap and there is a single value of  $\mu$  at which the film is electrically neutral and  $\delta N(E)$  is maximized.

The influence of disorder on the magnetoelectric response coefficient can be assessed qualitatively by considering a low-energy effective model for non-magnetic  $\mathbb{Z}_2$  TI thin films. We focus on  $\text{Bi}_2\text{Te}_3$  in the  $\text{X}_2\text{V}_3$  family of layered compounds for which such a model can be constructed using coupled Dirac-cones, one associated with the surface of each constituent layer [31, 32]. The parameters of the Dirac-cone model can be chosen to provide a semi-quantitative low-energy description [32, 33] of common magnetic and non-magnetic topological insulators and have the advantage of simplicity which allows the influence of an external magnetic field to be accounted for by explicit calculation. In these models, the linear response of electric polarization to magnetic field is contributed by the  $\mathcal{N} = 0$  anomalous Landau levels [30], whose wavefunctions are spatially polarized as illustrated in Fig. 3(a). The density-of-states versus band energy in the absence of disorder is plotted in Fig. 3 using black curves for the  $\mathcal{N} \neq 0$  contribution and red curves for the  $\mathcal{N} = 0$  contribution. In real materials, disorder is always present and, in the density of states, can be accounted for by convoluting with a finite-lifetime spectral function. The density-of-states calculated using Lorentzian broadening functions [33] is illustrated in Fig. 3(a) using dark green curves for weak disorder and orange dashed curves for strong disorder. In the presence of strong disorder, the anomalous Landau levels just below the Fermi level, which are localized near the bottom of the film in this illustration, are not fully occupied, and the anomalous Landau levels just above the Fermi level, which are localized near the top of the film, are not fully empty. The difference between the total densities in the top and bottom halves of the thin film is therefore reduced, as illustrated in Fig. 3(b). The end result is that disorder reduces the magnetoelectric response. Because the TME is an equilibrium and not a transport effect, precise quantization is not saved by disorder-induced localization even if it is

present.

*Discussion*— Although surface-state disorder does not save quantization of the TME, it may under some circumstances lead to interesting and informative noise and frequency dependencies in capacitive voltages measured in stacks similar to those in Fig. 1. We expect that magnetic noise and hysteresis associated with the single-surface magnetization reversals that separate QAH and axion insulator states will be amplified in the capacitive voltages because of the sensitivity of the TME to the relative orientations of top and bottom layer magnetizations. The change in charge distribution across the TI is in this case associated with rapid changes in the energy of the surface localized Landau level upon magnetization reversal. We expect that the time scale for equilibration when the magnetic field is changed within the narrow reversal intervals will normally be set by magnetic processes, whereas it will be set by electronic processes when the magnetic field is varied across the fixed magnetization axion insulator intervals. The response to magnetic field in these intervals accommodate changes in the surface state Landau level degeneracy, and moves charge between surfaces along the side walls. It is possible that this response will also be slow enough that its lag is observable if the surface states are strongly localized, leading to frequency-dependence in the capacitance.

In this Letter we have discussed measurement of the TME by capacitive detection of polarization response to magnetic field. It is also interesting to consider the possibility of probing the same quantity by measuring the orbital magnetization response to electric fields. Orbital magnetization can be measured directly by detection of the stray magnetic fields they produce [34–36]. It can also be measured indirectly by measuring Kerr magneto-optical response coefficients, and assuming that the two quantities are equivalent up to a separately measurable normalization factor. Assumptions of this nature are frequently made, but can be fully justified only when both quantities are linear in whatever parameter best characterizes time-reversal symmetry breaking – in the present case most likely the mean spin-polarization of the surface magnetic dopants. Since the TME is extremely non-linear in the absence of disorder, appearing instantly for infinitesimal time-reversal symmetry breaking, it seems unlikely that Kerr probes can be used for quantitative tests of the accuracy of TME quantization.

The TME can also be probed indirectly using transport. In the absence of disorder the TME of thin films with small surface magnetizations is equivalent to separate half-quantized surface state Hall conductivities of opposite signs on top and bottom film surfaces. Assuming that the two surfaces conduct in parallel, only one surface will contribute to the Hall conductivity when only one surface is magnetized. Its Hall conductivity can then be extracted by inverting the measured total resistivity. Indeed, experimental observation of a near half-quantized Hall effect has been reported in a thin film with magnetization on one surface only [37, 38]. This measured surface Hall conductivity implies that charge flows into or out of that surface as magnetic field is varied. Similarly, measure-

ments of the total QAH effect [39, 40] in thin films when the magnetization on the two surfaces are parallel can be viewed as providing information that is equivalent to that obtained by measurements in a device with only one magnetized surface. The Hall conductivity is simply twice as large as in the single-magnetic-surface case. The accuracy of quantization and the finite plateau width of the anomalous Hall effect, which is critical to identify quantized values, is assisted by disorder which makes states at the Fermi level in the 2-dimensional bulk irrelevant as long as they are localized. These surface localized states are not irrelevant for the TME in real disordered devices however, since they are related to the equilibrium charge transfer between layers after allowing the system to re-equilibrate following any change in the magnetic field value. The time scale required for this re-equilibration can be estimated by measuring the frequency-dependence of the capacitance in oscillating magnetic fields. The TME quantization should be more accurate when the magnetic field frequency exceeds the surface equilibration rate.

*Acknowledgements*— We acknowledge fruitful discussions with Cui-Zu Chang, Lingjie Zhou, Deyi Zhuo, and Xiaoda Liu. This work was supported by Welch Foundation grant F-2112 and by the Simons Foundation. C.M.C. acknowledges support from the Swedish Research Council (VR 2021-046229).

---

\* leichao.ph@gmail.com

- [1] X.-L. Qi, T. L. Hughes, and S.-C. Zhang, Topological field theory of time-reversal invariant insulators, *Phys. Rev. B* **78**, 195424 (2008).
- [2] X.-L. Qi and S.-C. Zhang, Topological insulators and superconductors, *Rev. Mod. Phys.* **83**, 1057 (2011).
- [3] M. Z. Hasan and C. L. Kane, Colloquium: Topological insulators, *Rev. Mod. Phys.* **82**, 3045 (2010).
- [4] R. S. K. Mong, A. M. Essin, and J. E. Moore, Antiferromagnetic topological insulators, *Phys. Rev. B* **81**, 245209 (2010).
- [5] D. Monaco and G. Panati, Symmetry and localization in periodic crystals: triviality of Bloch bundles with a fermionic time-reversal symmetry, *Acta Applicandae Mathematicae* **137**, 185 (2015).
- [6] D. Hsieh, D. Qian, L. Wray, Y. Xia, Y. S. Hor, R. J. Cava, and M. Z. Hasan, A topological Dirac insulator in a quantum spin Hall phase, *Nature* **452**, 970 (2008).
- [7] Y. Xia, D. Qian, D. Hsieh, L. Wray, A. Pal, H. Lin, A. Bansil, D. Grauer, Y. S. Hor, R. J. Cava, *et al.*, Observation of a large-gap topological-insulator class with a single Dirac cone on the surface, *Nature physics* **5**, 398 (2009).
- [8] Y. Chen, J. G. Analytis, J.-H. Chu, Z. Liu, S.-K. Mo, X.-L. Qi, H. Zhang, D. Lu, X. Dai, Z. Fang, *et al.*, Experimental realization of a three-dimensional topological insulator, *Bi2Te3*, *science* **325**, 178 (2009).
- [9] A. M. Essin, J. E. Moore, and D. Vanderbilt, Magnetolectric polarizability and axion electrodynamics in crystalline insulators, *Phys. Rev. Lett.* **102**, 146805 (2009).
- [10] A. M. Essin, A. M. Turner, J. E. Moore, and D. Vanderbilt, Orbital magnetolectric coupling in band insulators, *Phys. Rev. B* **81**, 205104 (2010).

- [11] J. Maciejko, X.-L. Qi, H. D. Drew, and S.-C. Zhang, Topological quantization in units of the fine structure constant, *Phys. Rev. Lett.* **105**, 166803 (2010).
- [12] S. Coh, D. Vanderbilt, A. Malashevich, and I. Souza, Chernsimons orbital magnetoelectric coupling in generic insulators, *Physical Review B* **83**, 085108 (2011).
- [13] K. Nomura and N. Nagaosa, Surface-quantized anomalous hall current and the magnetoelectric effect in magnetically disordered topological insulators, *Phys. Rev. Lett.* **106**, 166802 (2011).
- [14] H.-G. Zirnstein and B. Rosenow, Cancellation of quantum anomalies and bosonization of three-dimensional time-reversal symmetric topological insulators, *Phys. Rev. B* **88**, 085105 (2013).
- [15] M. Mulligan and F. J. Burnell, Topological insulators avoid the parity anomaly, *Phys. Rev. B* **88**, 085104 (2013).
- [16] A. Sekine and K. Nomura, Axion electrodynamics in topological materials, *Journal of Applied Physics* **129**, 10.1063/5.0038804 (2021).
- [17] J. Ahn, S.-Y. Xu, and A. Vishwanath, Theory of optical axion electrodynamics and application to the kerr effect in topological antiferromagnets, *Nature Communications* **13**, 7615 (2022).
- [18] T. Morimoto, A. Furusaki, and N. Nagaosa, Topological magnetoelectric effects in thin films of topological insulators, *Phys. Rev. B* **92**, 085113 (2015).
- [19] E. Witten, Fermion path integrals and topological phases, *Rev. Mod. Phys.* **88**, 035001 (2016).
- [20] P. T. Mahon, C. Lei, and A. H. MacDonald, Reconciling magnetoelectric response and time-reversal symmetry in non-magnetic  $\mathbb{Z}_2$  topological insulators (2023), [arXiv:2308.09282 \[cond-mat.mes-hall\]](https://arxiv.org/abs/2308.09282).
- [21] N. Pournaghavi, A. Pertsova, A. H. MacDonald, and C. M. Canali, Nonlocal sidewall response and deviation from exact quantization of the topological magnetoelectric effect in axion-insulator thin films, *Phys. Rev. B* **104**, L201102 (2021).
- [22] N. P. Armitage and L. Wu, On the matter of topological insulators as magnetoelectrics, *SciPost Phys.* **6**, 46 (2019).
- [23] F. Wilczek, Two applications of axion electrodynamics, *Phys. Rev. Lett.* **58**, 1799 (1987).
- [24] C.-Z. Chang, J. Zhang, X. Feng, J. Shen, Z. Zhang, M. Guo, K. Li, Y. Ou, P. Wei, L.-L. Wang, Z.-Q. Ji, Y. Feng, S. Ji, X. Chen, J. Jia, X. Dai, Z. Fang, S.-C. Zhang, K. He, Y. Wang, L. Lu, X.-C. Ma, and Q.-K. Xue, Experimental observation of the quantum anomalous hall effect in a magnetic topological insulator, *Science* **340**, 167–170 (2013).
- [25] Free excludes charges associated with dielectric discontinuities but includes the magnetic field induced charge associated with the TME.
- [26] P. Streda, Theory of quantised hall conductivity in two dimensions, *Journal of Physics C: Solid State Physics* **15**, L717 (1982).
- [27] P. Streda and L. Smrcka, Thermodynamic derivation of the hall current and the thermopower in quantising magnetic field, *Journal of Physics C: Solid State Physics* **16**, L895 (1983).
- [28] A. Widom, Thermodynamic derivation of the hall effect current, *Physics Letters A* **90**, 474 (1982).
- [29] A. H. MacDonald and P. Středa, Quantized hall effect and edge currents, *Phys. Rev. B* **29**, 1616 (1984).
- [30] C. Lei, P. T. Mahon, and A. H. MacDonald,  $\mathbb{Z}_2 = 0$  is topological too (2023), [arXiv:2311.17859 \[cond-mat.mes-hall\]](https://arxiv.org/abs/2311.17859).
- [31] A. Burkov and L. Balents, Weyl semimetal in a topological insulator multilayer, *Physical review letters* **107**, 127205 (2011).
- [32] C. Lei, S. Chen, and A. H. MacDonald, Magnetized topological insulator multilayers, *Proceedings of the National Academy of Sciences* **117**, 27224–27230 (2020).
- [33] Supplemental material, See Supplemental Material at [URL] for more information.
- [34] C. L. Tschirhart, M. Serlin, H. Polshyn, A. Shragai, Z. Xia, J. Zhu, Y. Zhang, K. Watanabe, T. Taniguchi, M. E. Huber, and A. F. Young, Imaging orbital ferromagnetism in a moiré chern insulator, *Science* **372**, 1323–1327 (2021).
- [35] S. Grover, M. Bocarsly, A. Uri, P. Stepanov, G. Di Battista, I. Roy, J. Xiao, A. Y. Meltzer, Y. Myasoedov, K. Pareek, K. Watanabe, T. Taniguchi, B. Yan, A. Stern, E. Berg, D. K. Efetov, and E. Zeldov, Chern mosaic and berry-curvature magnetism in magic-angle graphene, *Nature Physics* **18**, 885–892 (2022).
- [36] H. Zhou, N. Auerbach, M. Uzan, Y. Zhou, N. Banu, W. Zhi, M. E. Huber, K. Watanabe, T. Taniguchi, Y. Myasoedov, B. Yan, and E. Zeldov, Imaging quantum oscillations and millitesla pseudomagnetic fields in graphene, *Nature* **624**, 275–281 (2023).
- [37] M. Mogi, Y. Okamura, M. Kawamura, R. Yoshimi, K. Yasuda, A. Tsukazaki, K. S. Takahashi, T. Morimoto, N. Nagaosa, M. Kawasaki, Y. Takahashi, and Y. Tokura, Experimental signature of the parity anomaly in a semi-magnetic topological insulator, *Nature Physics* **18**, 390–394 (2022).
- [38] D. C. Ralph, Private communication, *Private Communication*.
- [39] E. J. Fox, I. T. Rosen, Y. Yang, G. R. Jones, R. E. Elmquist, X. Kou, L. Pan, K. L. Wang, and D. Goldhaber-Gordon, Part-per-million quantization and current-induced breakdown of the quantum anomalous hall effect, *Phys. Rev. B* **98**, 075145 (2018).
- [40] V. Dziom, A. Shuvaev, A. Pimenov, G. V. Astakhov, C. Ames, K. Bendias, J. Böttcher, G. Tkachov, E. M. Hankiewicz, C. Brüne, H. Buhmann, and L. W. Molenkamp, Observation of the universal magnetoelectric effect in a 3d topological insulator, *Nature communications* **8**, 15197 (2017).

### Supplementary Material for ‘‘Capacitive Detection of Topological Magneto-electric Effect’’

The Hamiltonian used in this work is constructed using Dirac cones that are coupled by hybridizing states:

$$\hat{H} = \sum_{\mathbf{k}_\perp, i, j, \mu, \gamma} \left[ \left( (-1)^i \hbar v_D (\hat{z} \times \boldsymbol{\sigma}) \cdot \mathbf{k}_\perp + m_i \sigma_z \right)_{\mu, \gamma} \delta_{ij} + \Delta_{ij} (1 - \delta_{ij}) \delta_{\mu, \gamma} \right] \hat{c}_{\mathbf{k}_\perp, i, \mu}^\dagger \hat{c}_{\mathbf{k}_\perp, j, \gamma}. \quad (7)$$

Here we have chosen  $\hat{z}$  as the stacking axis of topological insulator quintuple layers,  $\mathbf{k}_\perp = (k_x, k_y)$ ,  $i, j \in \{0, \dots, 2N - 1\}$  where  $i = 2(l - 1)$  ( $i = 2l - 1$ ) labels states that are associated with the bottom (top) surface of layer  $l \in \{1, \dots, N\}$ ,  $\mu, \gamma \in \{\uparrow, \downarrow\}$  are spin labels,  $\Delta_{ij}$  are the intra- and inter-layer hybridization parameters,  $v_D$  is the velocity of an isolated Dirac cone, and  $m_i$  are mass terms that account for exchange coupling to static local magnetic moments. The mass terms  $m_i$  are related to the magnetizations via the equation  $m_i = \sum_l J_{il} M_l$ , where  $M_l = 0$  for non-magnetic layers and  $\pm 1$  for magnetic layers; the Dirac-like states at the top or bottom surface of layer  $l$  are coupled to the static magnetization of that layer (via  $J_S$ ) and to that of the adjacent layer nearest that surface (via  $J_D$ ), and hybridized only to adjacent surfaces, with hopping  $\Delta_S$  for opposite surfaces of the same layer and  $\Delta_D$  for the closest surface of adjacent layers. When set the parameter  $J_D = J_S$ , this model describe the non-magnetic topological insulators with a surface magnetization  $J_S$ .

In the presence of an external magnetic field  $\mathbf{B} = -B\hat{z}$ , the  $\mathbf{k} \cdot \mathbf{p}$  model is mapped to an envelope function approximated Hamiltonian that is minimally-coupled to the electromagnetic field:  $\hbar\mathbf{k} \rightarrow -i\hbar\nabla - (eBx/c)\hat{y}$  in the Landau gauge. Here  $e$  is the elementary charge unit. Applying this recipe to Eq. (7) and seeking energy eigenvectors of the form  $\Psi_{E, q_y}(x, y) = e^{iq_y y} \Phi_{E, q_y}(x) / \sqrt{L_y}$ , where  $\Phi_{E, q_y}(x)$  has  $2N \times 2$  components that account for layer and spin label degrees of freedom,

$$H_D = \hbar v_D (\hat{z} \times \boldsymbol{\sigma}) \cdot \mathbf{k}_\perp \rightarrow \hbar \omega_c \begin{pmatrix} 0 & a^\dagger \\ a & 0 \end{pmatrix}, \quad (8)$$

where  $a = \frac{1}{\sqrt{2}}(\tilde{x} + \partial_{\tilde{x}})$  and  $a^\dagger = \frac{1}{\sqrt{2}}(\tilde{x} - \partial_{\tilde{x}})$  are Landau level raising and lowering (differential) operators,  $\omega_c \equiv v_D / \sqrt{2} l_B$ ,  $l_B \equiv \sqrt{\hbar c / eB}$  is the magnetic length, and  $\tilde{x} \equiv l_B q_y - x / l_B$ . The density of states in the presence of magnetic field is:

$$D(E) = \frac{eB}{h} \sum_{l=0}^{\infty} \delta(E - E_l), \quad (9)$$

where  $E_l$  is the Landau level energies. Considering the disorder effect, the density of states for Landau levels are broadened as:

$$D(E) = \frac{eB}{\pi h} \sum_{l=0}^{\infty} \frac{\Gamma}{\Gamma^2 + (E - E_l)^2}. \quad (10)$$

Here we considered a Lorentzian broadening where  $\Gamma$  is a parameter specifying the width which is determined by the strength of disorder. The projected integrated density of states to the top and bottom surface defined in the main text are calculated by

$$N_{i(b)}(E_F) = \sum_{i \leq N(i \geq N)} N_i(E_F) = \sum_{i \leq N(i \geq N)} \int_{-\infty}^{E_F} D(E) |\Phi_i(E_l)|^2 dE, \quad (11)$$

in which  $N$  is the thickness of thin films,  $E_F$  is the Fermi level, and  $i$  labels the Dirac cones locations. The  $\delta N(E) \equiv N_t(E_F) - N_b(E_F)$  is then used to characterize the electric polarization.